Ismail Yaqub Maolood, Yahya Eneid Abdulridha Al-Salhi, Songfeng Lu*

Thresholding for medical image segmentation for cancer using fuzzy entropy with level set algorithm

Abstract: In this study, an effective means for detecting cancer region through different types of medical image segmentation are presented and explained. We proposed a new method for cancer segmentation on the basis of fuzzy entropy with a level set (FELs) thresholding. The proposed method was successfully utilized to segment cancer images and then efficiently performed the segmentation of test ultrasound image, brain MRI, and dermoscopy image compared with algorithms proposed in previous studies. Results showed an excellent performance of the proposed method in detecting cancer image segmentation in terms of accuracy, precision, specificity, and sensitivity measures.

Keywords: Image segmentation; Fuzzy entropy; Level set algorithm; Thresholding cancer segmentation.

1 Introduction

Image segmentation is the partitioning of an image into several disjointed areas, particularly images with similar characteristics, such as color, texture, and intensity. Image segmentation is used in many fields, such as in cellular network architecture, color texturing based on an image segmentation system, and medical segmentation [1]. Image segmentation is extensively used in medical applications given its important role in image processing, especially in treatment progress monitoring, surgical planning, and abnormality detection [2]. Medical imaging is a discipline within the clinical field; this process involves using a technology to capture images of the internal parts of a human body [3]. These images are used in diagnostics as a teaching tool and in routine health care for various conditions. Medical imaging is typically referred to as diagnostic imaging because it is frequently used to aid doctors in formulating a diagnosis. Different types of technology are used in medical imaging at present. Medical image segmentation is aimed at identifying atomic structures, such as cysts, kidney tumor, skin cancer, brain tumor, and breast cancer, from images with remarkable abnormality [2]. This technique is difficult considering the various cancer sizes, shapes, and different types of the human body.

Many researchers have explored and proposed numerous methods for medical image segmentation. Masood et al. [3] merged clustering advantages with thresholding and proposed other modified methods for thresholding on the basis of fuzzy c-means (FCM) clustering for skin cancer detection. Wu, Weiwei, et al. [4] suggested an efficient semiautomatic method for segmentation of liver tumor in computed tomography (CT) volumes in accordance with the FCM with graph cuts. Padmapriya Nammalwar [5] developed a novel method that combines texture and color for skin lesions and segmentation from the natural skin area in the medical image. Patel Kinjal and Jasmine Jha [6] proposed a level set method with adaptive clustering techniques to segment multiple regions of a brain and identify the region with or without tumor. Minajagi and Goudar [7] proposed a discrete wavelet transform (DWT) and an FCM for the segmentation of a brain tumor MRI. Sonali Wadgure and Pooja Thakre [8] established a fuzzy level set algorithm for medical image segmentation of a brain. Aja-Fernández et al.[9] presented a new multi-region thresholding method for images that are corrupted

*Corresponding author: Songfeng Lu, School of Computer Science and Technology, Huazhong University of Science and Technology, Wuhan, 430074, China
Shenzhen Huazhong University of Science and Technology Research Institute, Shenzhen, 518063, China. lusongfeng@hust.edu.cn ; Tel.: +86-13971398213.
Ismail Yaqub Maolood, Yahya Eneid Abdulridha Al-Salhi, School of Computer Science and Technology, Huazhong University of Science and Technology, Wuhan, 430074, China

with noise and artifacts to a multi-region image segmentation. Mirza et al.[10] presented a new water flow-like algorithm with fuzzy entropy for efficiency and accuracy of an MRI image segmentation.

2 Methods

In this section, we discuss our study techniques for searching and identifying the cancer region to segment into different types of medical images. The process of the proposed method is as follows.

2.1 Selection cancer region based on a level set algorithm

In 1987, Osher and Sethian introduced a level set method, which utilizes and implements the dynamic variation boundary for medical image segmentation. Most medical image modalities are grayscale, and $m = (x, y)$ is considered a point in the medical image. This point and the position of $m(t)$ will evolve at the overtime. t is the time for the $m(t)$ point on the surface; this point is expressed below [22].

$$\emptyset(m(t), t) = 0 \qquad (1)$$

The boundary segmentation for the medical image is defined as a part surface where the contour level set equals zero. The height surface is equal to the length from $m = (x, y)$ to the nearest point on the contour [23].

$$\emptyset(x, y, t = 0) = \pm d \qquad (2)$$

Where x and y are the points on the image, t is the time, and d is the distance between x, y point and zero level set. The partial differential equations (PDE) function $\emptyset(x, y, t = 0)$, and evaluation is possible by approximating the active contours by tracking zero level set for point and position of overtime $m(t)$. The development of a curved surface is characterized by the various forces of the internal and external research archives. The height surface is equal to the distance from the nearest pixel on an active contour to (x, y), such that $\emptyset(t, x, y,) < 0$, the initial function $\emptyset$ with distance $m(t)$ being negative inside the contour, if $\emptyset(t, x, y,) > 0$, the initial function $\emptyset$ with $m(t)$ is positive outside the contour, and if $\emptyset(t, x, y,) \cong 0$, the initial function $\emptyset$ of the level set matches the initial contour are getting closer to the target boundaries of cancer, the speed function is expected to gradually slow down to zero.

[24]. The distance value of d outside the curve is positive, whereas the distance value of d inside the contour is negative; furthermore, the distance value of d on the boundary of the image is equal to zero [24]. The initial function $\emptyset$ can be the arbitrary function until the zero level set equals the initial contour. Thus, initial function $\emptyset = t = 0$ or $\emptyset t$ is overtime, and we can use motion equation $\frac{\partial \emptyset}{\partial t}$ with the chain rule.

$$\frac{\partial \emptyset(m(t), t)}{\partial t} = 0$$

$$\frac{\partial \emptyset}{\partial m(t)} \frac{\partial m(t)}{\partial t} + \frac{\partial \emptyset}{t} \frac{t}{t} = 0 \qquad (3)$$

$$\frac{\partial \emptyset}{\partial m(t)} m_t + \emptyset_t = 0$$

If the motion equation is $\frac{\partial \emptyset}{\partial t} = \nabla \emptyset$, and $m(t)$ is the speed of normal force F to the surface, then $m(t) = F(m(t))n$, where n equals $\frac{\nabla \emptyset}{|\nabla \emptyset|}$. The motion equation is $\frac{\partial \emptyset}{\partial t}$. The advancing force F must be regularized by an edge indication initial function $\emptyset_t$ to stop the level set evolution near the optimal solution [24]. The equation can be rewritten as.

$$\emptyset_t + \nabla \emptyset m_t = 0$$

$$\emptyset_t + \nabla \emptyset Fn = 0$$

$$\emptyset_t + F \nabla \emptyset \frac{\nabla \emptyset}{|\nabla \emptyset|} = 0 \qquad (4)$$

$$\emptyset_t + F|\nabla \emptyset| = 0$$

$t = 0$ is the time for the process, and defining the overtime for a motion to $\emptyset(x, y, t)$ at any time t by evolving the initial $\emptyset(x, y, t = 0)$ overtime is possible after defining the motion of $\emptyset$ in Eq. 4. The surface curvature by motion $\emptyset$ and a popular formulation for the level set method to find the part with cancer can be obtained by.

$$k = \nabla \frac{\nabla \emptyset}{|\nabla \emptyset|} = \frac{\emptyset_{xx}\emptyset_y^2 - 2\emptyset_{xy}\emptyset_x\emptyset_y + \emptyset_{yy}\emptyset_x^2}{\left(\emptyset_x^2 + \emptyset_y\right)^{1/2}} \qquad (5)$$

2.2 Medical cancer thresholding based on fuzzy entropy

Thresholding method is a technique that uses the classification pixels to segment colored and grayscale images. Many methods, such as scene processing, medical thresholding, document image analysis, and map processing have been proposed for image thresholding application. The simplest method for medical

image segmentation is the image thresholding technique; this technique is the simplest method for implementing an image and thus accelerates the process. $D = (i, j)$, where $i = (0, 1 \ldots M - 1)$, $j = (0, 1 \ldots N - 1)$. In these variables, M and N are two integer numbers that correspond to the width and height of a medical image. $G = (0, 1 \ldots L - 1)$ is used to determine the number of grayscale in a medical image. $I(x, y)$ is adopted to obtain the grayscale value of an image at a pixel (x, y), and $DK = (x, y)$; moreover $I(x, y) = k$, where $(x, y) = D$ and $k = (0, 1, \ldots, L - 1)$. We suggest that $T1$ and $T2$ be utilized as the thresholds for medical image segmentation; D is an original medical image domain and divided into three regions, namely, E_m, E_b, and E_d. The E_d region covers the pixels with less grayscale value than $T1$, E_m covers the pixels with a middle grayscale value between $T1$ and $T2$, and E_b covers the pixels with more grayscale value than $T2$. $W_3 = E_m, E_b,$ and E_d is the unknown probabilistic distribution of D domain, which probability distribution is described in [25, 27].

$$pd = P(E_d)$$

$$pm = P(E_m) \quad (6)$$

$$pb = P(E_b)$$

The membership functions (μ) for $E_d, E_m,$ and E_b correspond to $\mu_m, \mu_b,$ and μ_d and requires six parameters for this process, that is, $a1, b1, c1, a2, b2,$ and $c2$. In accordance with the membership function (μ), the thresholds $T1$ and $T2$ are the variables for every pixel $k = 0, 1, \ldots, 255$ [26, 27].

$$D_d = \{(x, y): I(x, y) \leq T1, \ (x, y) \in D_k\}$$

$$D_m = \{(x, y): T1 < I(x, y) \leq T2, \ (x, y) \in D_k\} \quad (7)$$

$$D_b = \{(x, y): I(x, y) > T2, \ (x, y) \in D_k\}$$

The condition of a probability of $E_m, E_b,$ and E_d to $p_{m|k}, p_{b|k},$ and $p_{d|k}$ of a pixel is divided into three classes, namely, dust, bright, and dark. The pixel pertains to D_k with $p_{m|k} + p_{b|k} + p_{d|k} = 1$, $k = 0, 1, 2 \ldots 255$. then, the abovementioned equation can be rewritten as.

$$P_{km} = P(D_d) = P_k * P_{m|k}$$

$$P_{kb} = P(D_m) = P_k * P_{b|k} \quad (8)$$

$$P_{kd} = P(D_b) = P_k * P_{d|k}$$

The grayscale value with a grade of pixels for k among

the classes of dust (E_m), bright (E_b), and dark (E_d) can be determined as equivalent to the condition of the probabilities $p_{m|k}, p_{b|k},$ and $p_{d|k}$. The equation can be expressed as.

$$P_m = \sum_{k=0}^{255} P_k * P_{m|k} = \sum_{k=0}^{255} P_k * \mu_m(k)$$

$$P_b = \sum_{k=0}^{255} P_k * P_{b|k} = \sum_{k=0}^{255} P_k * \mu_b(k) \quad (9)$$

$$P_d = \sum_{k=0}^{255} P_k * P_{d|k} = \sum_{k=0}^{255} P_k * \mu_d(k)$$

We selected the three parameters for fuzzy membership function, that is, $U, S,$ and Z, where $U = (k, a1, b1, c1, a2, b2, c2)$, $S(k, a1, b1, c1, a2, b2, c2)$, and $Z(k, a1, b1, c1, a2, b2, c2)$ as the membership function classes of dust $\mu_m(k)$, bright $\mu_b(k)$, and dark $\mu_d(k)$ [25, 26, 28]. The three equations for membership functions can be rewritten as.

$$\mu_m(k) = \begin{cases} 0, & k \leq a1 \\ \dfrac{(k - a1)^2}{(c1 - a1) * (b1 - a1)}, & a1 < k \leq b1 \\ 1 - \dfrac{(k - c1)^2}{(c1 - a1) * (c1 - b1)}, & b1 < k \leq a2 \\ 1, & c1 < k \leq a2 \\ 1 - \dfrac{(k - a2)^2}{(c2 - a2) * (b2 - a2)}, & a2 < k \leq b2 \\ \dfrac{(k - c2)^2}{(c2 - a2) * c2 - b2)}, & b2 < k \leq c2 \\ 0, & k > c2 \end{cases} \quad (10)$$

$$\mu_b(k) = \begin{cases} 0, & k \leq a2 \\ \dfrac{(k - a2)^2}{(c2 - a2) * (b2 - a2)}, & a2 < k \leq b2 \\ 1 - \dfrac{(k - c2)^2}{(c2 - a2) * (c2 - b2)}, & b2 < k \leq c2 \\ 1, & k > c2 \end{cases} \quad (11)$$

$$\mu_d(k) = \begin{cases} 1, & k \leq a1 \\ 1 - \dfrac{(k - a1)^2}{(c1 - a1) * (c1 - b1)}, & a1 < k \leq b1 \\ \dfrac{(k - c1)^2}{(c1 - a1) * (c1 - b1)}, & b1 < k \leq c1 \\ 0, & k > a1 \end{cases} \quad (12)$$

The six parameters must be within the range of $(0 \leq a1 < b1 < c1 < a2 < b2 < c2 \leq 255)$ pixels. The function of fuzzy entropy for each class of dust, bright, and dark is defined as.

$$H_m = -\sum_{k=0}^{255} \frac{P_k * \mu_m(k)}{P_m} * \ln\left(\frac{P_k * \mu_m(k)}{P_m}\right)$$

$$H_b = -\sum_{k=0}^{255} \frac{P_k * \mu_b(k)}{P_b} * \ln\left(\frac{P_k * \mu_b(k)}{P_b}\right) \quad (13)$$

$$H_d = -\sum_{k=0}^{255} \frac{P_k * \mu_d(k)}{P_d} * \ln\left(\frac{P_k * \mu_d(k)}{P_d}\right)$$

The total fuzzy entropy function for all classes can be computed and summarized.

$$H\{(c1, a2), (b2, c2), (a1, b1)\} = H_m + H_b + H_d \quad (14)$$

The objective functions of the abovementioned equation apply optimization techniques to find the maximum value of fuzzy entropy for all classes. The threshold technique is calculated using the following equation.

$$\mu_d(T1) = \mu_m(T1) = 0.5$$
$$\mu_m(T2) = \mu_b(T2) = 0.5 \quad (15)$$

On the basis of Eqs. (10–12), the thresholds T1 and T2 are considered the points of intersection for dust $\mu_m(k)$, bright $\mu_b(k)$, and dark $\mu_d(k)$. T1 and T2 can be calculated as follows.

$$T1 =
\begin{cases}
a1 + \sqrt{\dfrac{(c1-a1)*(b1-a1)}{2}}, & \dfrac{(a1+c1)}{2} \leq b1 \leq c1 \\[4mm]
c1 - \sqrt{\dfrac{(c1-a1)*(c1-b1)}{2}}, & a1 \leq b1 \leq \dfrac{(a1+c1)}{2}
\end{cases}$$

$$T2 =
\begin{cases}
a2 + \sqrt{\dfrac{(c2-a2)*(b2-a2)}{2}}, & \dfrac{(a2+c2)}{2} \leq b2 \leq c2 \\[4mm]
c2 - \sqrt{\dfrac{(c2-a2)*(c2-b2)}{2}}, & a2 \leq b2 \leq \dfrac{(a2+c2)}{2}
\end{cases} \quad (16)$$

2.3 Proposed method approach

Numerous researchers have worked and developed methods for solving cancer problems by using medical image segmentation. The proposed method is used to find multiple cancers in different medical images and conduct estimation analyses of these cancers. The goal of the proposed method is to output useful information for cancer boundary through medical image segmentation and be efficient in classifying cancer. This study also attempts to combine several methods to create an effective segmentation. A flowchart of this process is illustrated in Figure 1.

Our FELs thresholding proposed algorithm

Input: Medical image.
Output: Extracted the part with cancer and then segmented.
Step 1: Read medical image.
Step 2: Create a loop for reading the pixels of a medical image.
Step 3: Initiate counter searching of a medical image in accordance with Eq. (4). If the force is positive (F =1), then the counter must be from inside the image. If the force is negative (F=–1), then the force must be outside the counter.
Step 4: Evaluate the function $\emptyset$ by the numerical level set using Eqs. (2 and 3).
Step 5: If the function $\emptyset_t$ is approximately zero in a boundary by Eq. (4), then proceed to the next equation to select the part with cancer tissue range.

$$k = \nabla \frac{\nabla\emptyset}{|\nabla\emptyset|} = \frac{\emptyset_{xx}\emptyset_y^2 - 2\emptyset_{xy}\emptyset_x\emptyset_y + \emptyset_{yy}\emptyset_x^2}{(\emptyset_x^2 + \emptyset_y^2)^{1/2}}$$

Step 6: Define the three parameters for fuzzy entropy membership functions, such as U, S, and Z, to initialize the membership function values, namely, dust $\mu_m(k)$, bright $\mu_b(k)$, and dark $\mu_d(k)$, using Eqs. (10–12), respectively.
Step 7: Calculate double thresholding to find the lower and upper limits using Eq. (15).
Step 8: Extract the part with cancer and segment the medical image in accordance with Eq. (16).
Step 9: End.

This flowchart demonstrates the proposed method for a cancer region through medical image segmentation. This method consists of the following three stages: the first stage is using a level set algorithm to search in a medical image to find the part with cancer and select it. The second stage is using the fuzzy entropy to experiment and analyze the part with cancer and segment it after the selected previews of the algorithm. The final stage is using double thresholding to extract the part with cancer. The details of the proposed method are presented as follows.

1. The level set algorithm creates a loop to search for the medical image and find the parts with cancer tissue region and select it.

2. The background and foreground regions are calculated for every threshold grayscale level.

3. The pixels of the membership degree of the medical image are calculated for every threshold grayscale level.

4. The fuzzy entropy algorithm is calculated for every threshold grayscale level, and the smallest value of the threshold is selected.

5. The part with cancer is a threshold with the grayscale level based on the smallest value of the fuzzy entropy.

6. The cancer region is segmented and extracted.

3 Results and discussion

In this study, we present and apply the proposed segmentation result for medical image problems. The proposed algorithm has been applied to 84 images and is divided into three types of images, in which 28 images are ultrasound for breast cancer, 32 images are brain MRI, and 24 images are dermoscopy color image. The FELs thresholding method has been implemented in the three types of the medical image affected by three types of cancer. Cancer may be large, medium, or small. Our study consists of three stages. The first stage confirms the effectiveness, efficiency, and accuracy of our study by comparing it with the three other algorithms used for medical image segmentation [31-33]. The second part explains the capability of our method in terms of efficiency. The final stage implements and evaluates the proposed method for medical image segmentation of cancer. All methods are implemented by MATLAB2014a on a computer with CPU 3.50 GHz and 8 GB RAM and the operating system is 64-bit Windows 7.

3.1 Experiment the results

In this study, we present and explain the analysis of results with the initial counter that utilizes the FELs thresholding algorithm. The analysis is conducted by using three types of medical image, that is, ultrasound for breast cancer, brain MRI, and dermoscopy skin image. The results of the experiment show that the compact constraint of the proposed method exerts various effects on different degrees of compactness. Figures (2–4)a depict the original images. The searching and scanning have started to find the ground truth (GT) regions of cancer by decreasing and increasing the parameter value of the mask (M), as demonstrated in Figures (2–4)b; these processes continue pixel by pixel on the medical image until the nearest GT boundary of cancer. The level set method creates a red initial curve around the cancer region because this method is sensitive to this process, as displayed in Figures (2–4)c. The experimental images illustrated optimization steps of iterations until achevieing the optimum solution which showed the results in Figures 5, 6 and 7. Table 1 and Figure 8 summarize the performance of the FELs thresholding method, which is calculated for sensitivity, precision, specificity, and accuracy measures, for each medical image.

3.2 Segmentation result and comparison

The proposed (FELs) thresholding method is used in the experiment and test conducted on the three types of medical image to find the boundaries of the cancer
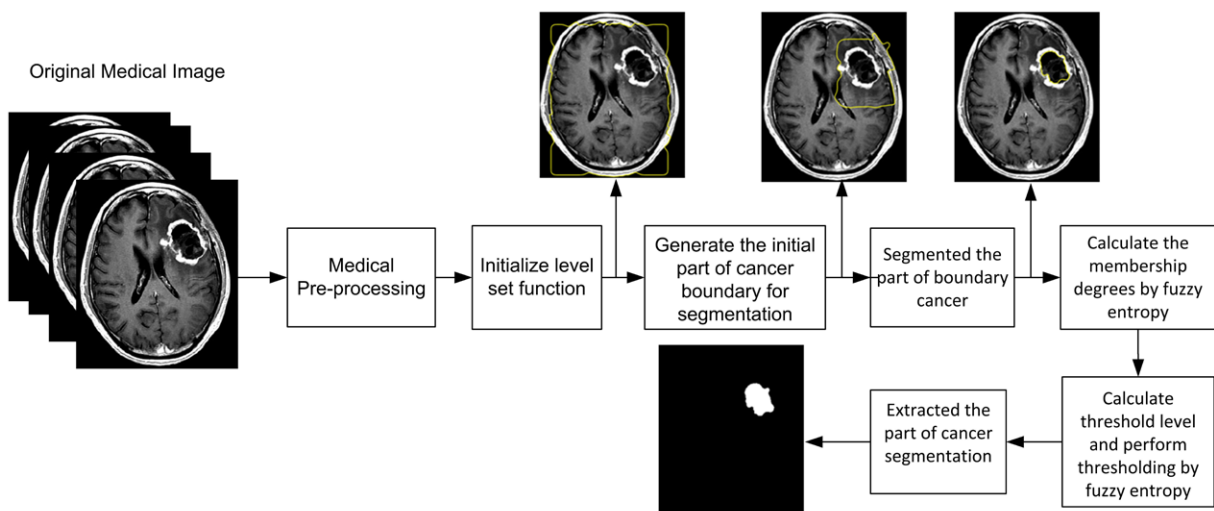

Figure 1: Proposed approach for extracting the part with cancer through medical image segmentation.
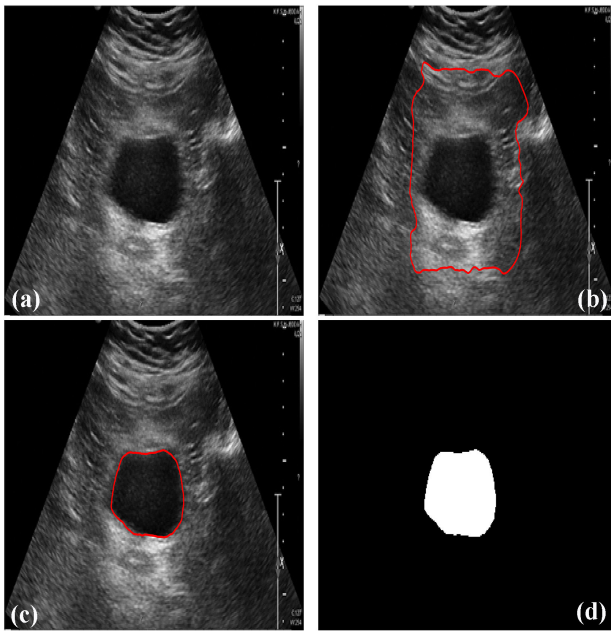
Figure 2: Fuzzy entropy with level set segmentation of ultrasound breast cancer: (a) Original ultrasound image with cancer, (b) is searching to find the cancer to region, (c) find the cancer and segmented after 130 iterations, (d) is initialization by thresholding (100-220,250-340) for extracted the cancer region.
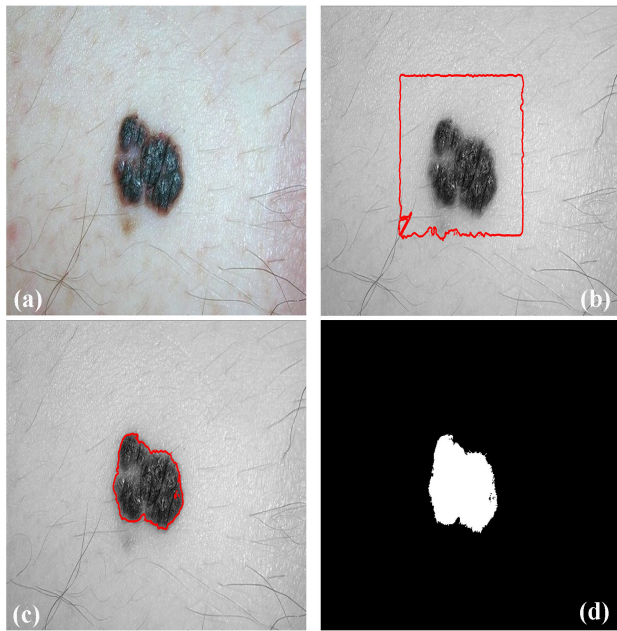

Figure 4: Fuzzy entropy with level set segmentation of dermoscopy color image for skin cancer: (a) Original skin image with cancer, (b) is searching to find cancer to region, (c) find the cancer and segmented after 300 iterations, (d) is initialization by thresholding (120-230,170-310) for extracted the cancer region.
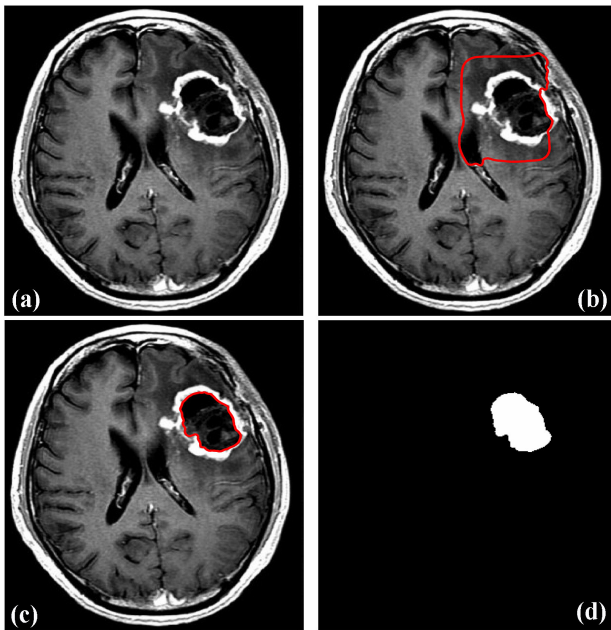

Figure 3: Fuzzy entropy with level set segmentation of MRI Brain cancer: (a) Original MRI image with cancer, (b) is searching to find the cancer to region, (c) find the cancer and segmented after 130 iterations, (d) is initialization by thresholding (80-170,170-230) for extracted the cancer region.

Figure 5: Illustrates iteration measures in ultrasound breast cancer segmentation.

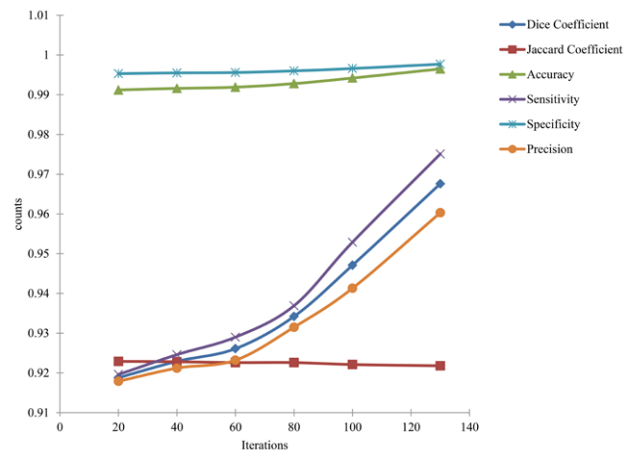regions; the results are segmented and extracted, and the (FELs) thresholding method is compared with the different segmentation methods for cancer. In 1945, Dice intro-duced a Dice coefficient method [29] and in 1912, Taccard introduced a Jaccard coefficient method [30], which utilizes for computing of the extent of spatial overlap between two binary images. It is commonly used in reporting to evaluate and perform the part of cancer segmentation or registration effects which can measure the overlap with the ground truth image. They can range between 0 (no overlap) and 1 (perfect agreement). Dice and Jaccard similarity coefficients are computed by measuring the similarity of the pixels in terms of the GT and cancer seg-
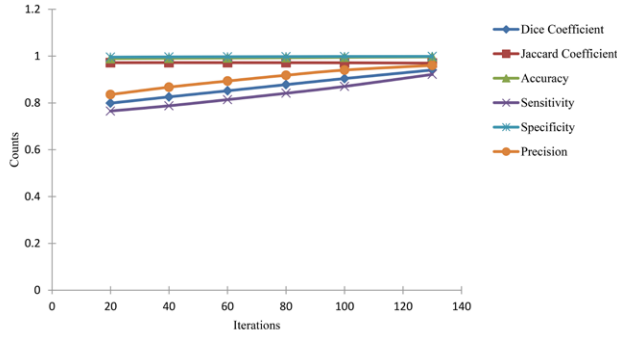
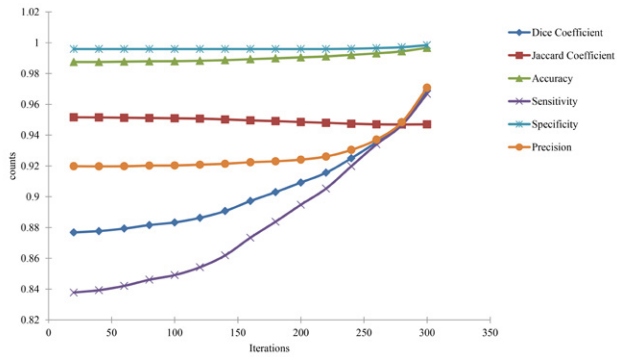**Figure 6:** Shows iteration measures in brain cancer segmentation.

Figure 7: Shows iteration measures of dermoscopy color image in skin cancer segmentation.

Table 1: Results of cancer segmentation by FELs proposed methods for medical image.

Medical Image	Ultrasound Image	MRI Image	Dermoscopy Image
Jaccard Coefficient	0.9229	0.9718	0.9515
Dice Coefficient	0.9187	0.7989	0.8768
Accuracy	0.9912	0.9892	0.9875
Sensitivity	0.9196	0.7653	0.8378
Specificity	0.9953	0.9956	0.9959
Precision	0.9179	0.8357	0.9198
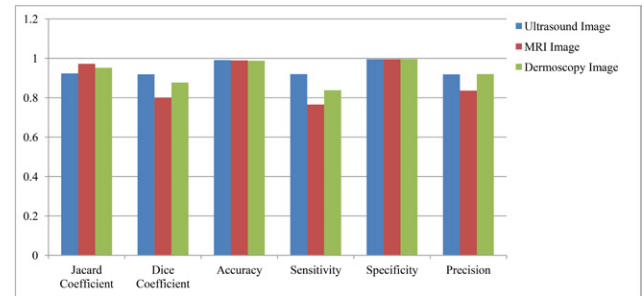
Figure 8: Results of performance measures segmentation for FELs proposed methods for medical image.

mentation (CS) [31]. The performance of CS calculated by four factors is utilized. A true positive pixel indicates an existing and accurately detected cancer region, whereas a false positive pixel denotes a non-existing cancer case, but a result is detected. A true negative pixel indicates a non-existing cancer case, and the result is undetected, whereas a false negative pixel denotes an existing cancer case, but the result is undetected [33]. The parameter details are provided mathematically as follows:

Jaccard similarity: GT represents ground truth, and CS denotes cancer segmentation; Jaccard coefficient is defined as follows:

$$\text{Jaccard coefficient} = \frac{|GT \cap CS|}{|GT \cup CS|} \qquad (17)$$

Dice similarity coefficient shows that.

$$\text{Dice coefficient} = \frac{2 * |GT * CS|}{|GT| + |CS|} \qquad (18)$$

Where CS is the cancer segmentation and GT is the ground truth image. The results showed that Jaccard and Dice coefficient was in between 0 and 1. The value of 0 corresponds to no similarity (no overlap), whereas the value of 1 indicates a similarity (perfect agreement). According

to the results, Jaccard coefficient is implementing better than Dice coefficient for cancer segmentation. We test the proposed (FELs) thresholding method to measure the capability of the method in terms of sensitivity, precision, specificity, and accuracy measures by checking the negative CS results, positive CS results, positive predictive pixel values, and true CS results [33].

$$\text{Sensitivity} = \frac{TP}{TP + FN} \qquad (19)$$

$$\text{Precision} = \frac{TP}{TP + FP} \qquad (20)$$

$$\text{Specificity} = \frac{TN}{TN + FP} \qquad (21)$$

$$\text{Accuracy} = \frac{TP + TN}{TP + TN + FP + FN} \qquad (22)$$

The accuracy results are defined as "correct" if the medical image is segmented correctly. If only a part of this region is segmented correctly, then the results are defined as "poor" results. To emphasize the accuracy results, we use the correct and poor rates, which are defined as

$$\text{Correct Rate} = (X\text{correct} / X) * 100\% \qquad (23)$$

$$\text{Poor Rate} = (X\text{Poor} / X) * 100\% \qquad (24)$$

Table 2: Comparison of our proposed method with other standard methods in terms of Dice coefficient and, Jaccard coefficient.

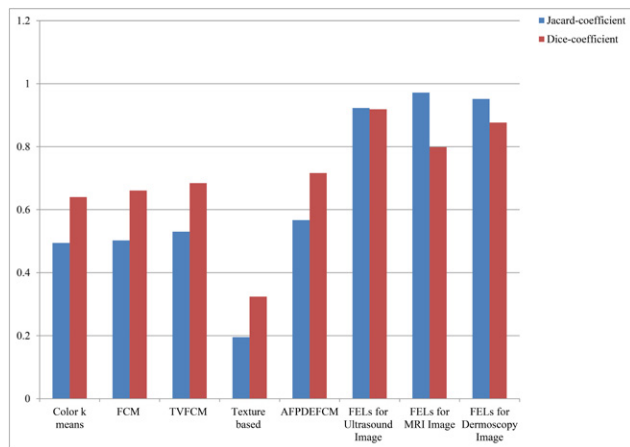| Cancer segmentation method	Performance measures for segmentation	
	Jaccard - coefficient	Dice -coefficient
Color k means	0.494357	0.640071
FCM	0.502415	0.660864
TVFCM	0.530086	0.684207
Texture based	0.195247	0.324119
AFPDEFCM	0.566755	0.716681
FELs for Ultrasound Image	0.922922	0.918703
FELs for MRI Image	0.971831	0.798921
FELs for Dermoscopy Image	0.951513	0.876811

Figure 9: Comparison the performance measures segmentation for our proposed method with other standard segmentation cancer methods according to Dice-coefficient, and Jaccard-coefficient.

Where X is the total number of medical images. The FELs thresholding method has been applied to 84 images and divided into three types of medical images to determine the accuracy of the cancer image. The proposed method provides a correct rate of 96.4% and a poor rate of 3.6% after detecting 27 cancer cases from 28 ultrasound results for breast cancer; the correct rate of 96.9% and poor rate of 3.1% are obtained after detecting 31 cancer cases from 32 MRI brain cancer results; the correct rate of 95.8% and poor rate of 4.2% are achieved after detecting 23 cancer cases from 24 dermoscopy image results. The proposed algorithm has performed well and obtained a better result than the other approaches [32, 33]. Table 2 summarizes the comparison of the results.

Also, besides the cancer region, they have other types of the pathological lesion and a similar signal as
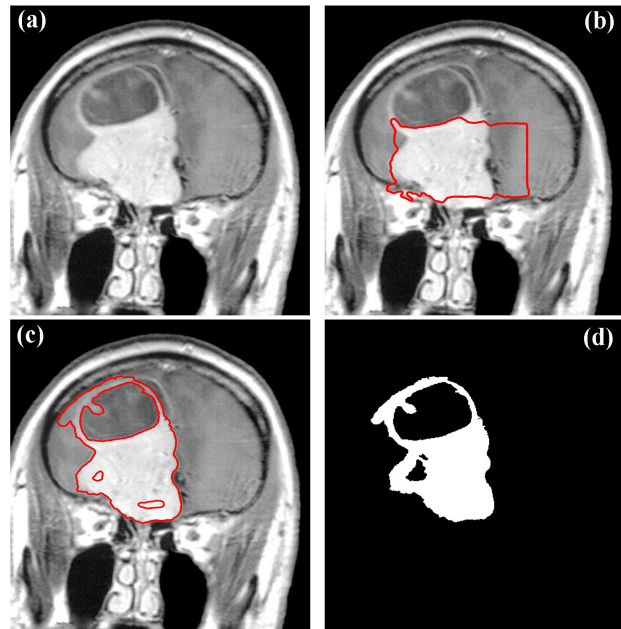

Figure 10: Traumatic brain injury (TBI) with cancer, (a) Original image, (b) searching for injury with cancer, (c) find injury with cancer and segmented, (d) Thresholding and extracted the injury with cancer region.
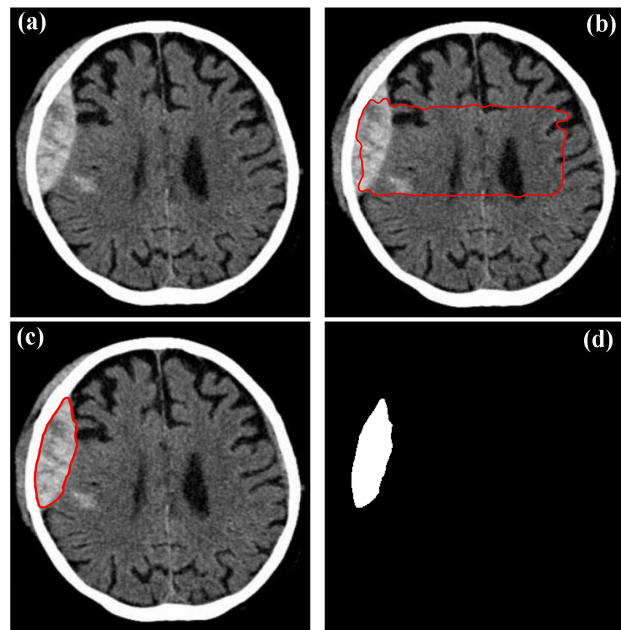

Figure 11: Traumatic brain injury (TBI), (a) Original image, (b) searching for injury, (c) find injury and segmented, (d) Thresholding and extracted the injury region.

the cancer region, such as traumatic brain injury (TBI). The study have applied (FELs) thresholding method to TBI image. According to the equations (19, 21 and 22) pro-

vided earlier, it might be possible to achieve the satisfied outcome as explained below:

Figures 10 and 11 show pathological lesions and similar to signal of the cancer region. The testing results for figure10 according to equations (1, 2 and 3) for sensitivity; specificity; and accuracy were (0, 0.2028, 0) respectively. Also for figure 11was (0, 0.2869, 0) respectively.

4 Conclusion

The proposed FELs threshold method can be beneficial to developing a system for clinical images used for diagnoses. In this method, three types of images such as ultrasound results for breast cancer, brain MRI, and dermoscopy skin image. The proposed method achieved 92.29%, 97.18%, and 95.15% for the Jaccard similarity coefficient whereas 91.87%, 79.89%, and 87.68% for the Dice similarity coefficient, respectively. The Jaccard and Dice similarity coefficients are utilized to compare the diversity and similarity pixels between the images. The proposed method indicates a favorable accuracy for cancer detection through each medical image segmentation that we used in a computer-aided diagnosis. The computational costs are disregarded because the detection rate has reached a favorable degree. The successful rate of the FELs thresholding method indicates each medical image at 0.9912, 0.9892, and 0.9875 for accuracy; 0.9196, 0.7653, and 0.8378 for sensitivity; 0.9953, 0.9956, and 0.9959 for specificity; 0.9179, 0.8357, and 0.9198 for precision, correspondingly. The accuracy degree for detecting cancer in patients through the medical image segmentation is promising. This method can be utilized to classify the type of cancers in accordance with the clinical diagnosis method. Future work is planned to optimize our algorithm to be able to detect the non-brain original cancer metastasis.

Conflict of interest: The authors report no conflicts of interest in this work.

References

[1] Khelifi L., Mignotte M., EFA-BMFM: A multi-criteria framework for the fusion of colour image segmentation, Information Fusion., 2017, 38,104-121

[2] Gui L., Li C., Yang X., Medical image segmentation based on level set and isoperimetric constraint, Physica Medica: European Journal of Medical Physics., 2017, 42, 162-173

[3] Chen Y.T., A novel approach to segmentation and measurement of medical image using level set methods, Magnetic resonance imaging., 2017, 39, 175-193

[4] Masood A., Al-Jumaily A. A., Maali Y., Level Set Initialization Based on Modified Fuzzy C Means Thresholding for Automated Segmentation of Skin Lesions, In International Conference on Neural Information Processing, Springer, Berlin, Heidelberg., 2013, 341-351

[5] Wu W., Wu S., Zhou Z., Zhang R., Zhang Y., 3D Liver Tumor Segmentation in CT Images Using Improved Fuzzy C-Means and Graph Cuts, BioMed research international., 2017

[6] Patel K., Jha J., Brain tumor image segmentation using adaptive clustering and level set method, image., 2014, 9.

[7] Minajagi P.B., Goudar R. H., Segmentation of Brain MRI Images using Fuzzy C-Means and DWT, 2016

[8] Wadgure S., Thakre P., Detection of Brain Tumor from MRI of Brain Using Fuzzy C-Mean (FCM), International Journal of Science, Engineering and Technology Research (IJSETR)., 2014, 8

[9] Dey N., Rajinikanth V., Ashour A. S., Tavares J. M., Social Group Optimization Supported Segmentation and Evaluation of Skin Melanoma Images, Symmetry., 2018, 10-51

[10] Aja-Fernández S., Curiale A. H., Vegas-Sánchez-Ferrero G., A local fuzzy thresholding methodology for multiregion image segmentation, Knowledge-Based Systems., 2015, 83, 1-2

[11] Mirzad S. A., Vahidi J., Hamedi S. M., Automatic MRI image segmentation using water flow like algorithm and fuzzy entropy, In Knowledge-Based Engineering and Innovation (KBEI), 2015. 2nd International Conference of the IEEE., 2015, 223-226

[12] Yeniyayla Y., Fuzzy entropy and its application, PhD dissertation, DEÜ Fen Bilimleri Enstitüsü., 2011

[13] Dhar M., Chutia R., Mahanta S., A note on existing Definition of Fuzzy Entropy, International Journal of Energy Information and Communications., 2012, 3,17-21

[14] Qi C., Maximum entropy for image segmentation based on an adaptive particle swarm optimization, Applied Mathematics and Information Sciences., 2014, 8, 31-29

[15] Jaganathan P., Kuppuchamy R., A threshold fuzzy entropy based feature selection for medical database classification, Computers in Biology and Medicine., 2013, 43, 2222-2229.

[16] Sanyal N., Chatterjee A., Munshi S., An adaptive bacterial foraging algorithm for fuzzy entropy based image segmentation, Expert Systems with Applications., 2011, 38, 15489-15498

[17] Baâzaoui A., Barhoumi W., Ahmed A., Zagrouba E., Semi-automated segmentation of single and multiple tumors in liver CT images using entropy-based fuzzy region growing, IRBM., 2017, 38, 98-108

[18] Brox T., Weickert J., Level set segmentation with multiple regions, IEEE Transactions on Image Processing., 2006, 15, 3213-3218

[19] Pham T. X., Siarry P., Oulhadj H., Integrating fuzzy entropy clustering with an improved PSO for MRI brain image segmentation, Applied Soft Computing., 2018, 65, 230-242

[20] Peng D., Merriman B., Osher S., Zhao H., Kang M., Fronts propagating with curvature-dependent speed: algorithms based on hamilton-jacobi formulation, Journal of Computational Physics., 1999, 155, 410-438

[21] Li B. N., Chui C. K., Chang S., Ong S. H., Integrating spatial fuzzy clustering with level set methods for automated medical image segmentation, Computers in biology and medicine., 2011, 41, 1-0

[22] Agarwal P., Kumar S., Singh R., Agarwal P., Bhattacharya M., A combination of bias-field corrected fuzzy c-means and level set approach for brain MRI image segmentation, InSoft Computing and Machine Intelligence (ISCMI), 2015. Second International Conference of the IEEE., 2015, 84-87

[23] Chen T.F., Medical image segmentation using level sets, Technical Report. Canada, University of Waterloo., 2008, 1-8

[24] Gharipour A., Liew A. W., An integration strategy based on fuzzy clustering and level set method for cell image segmentation, InSignal Processing, Communication and Computing (ICSPCC), 2013. IEEE International Conference., 2013, 1-5

[25] Tao W. B., Tian J. W., Liu J., Image segmentation by three-level thresholding based on maximum fuzzy entropy and genetic algorithm, Pattern Recognition Letters., 2003, 24, 3069-3078

[26] Tao W., Jin H., Liu L., Object segmentation using ant colony optimization algorithm and fuzzy entropy, Pattern Recognition Letters., 2007, 28, 788-796

[27] Naidu M. S., Kumar P.R., Chiranjeevi K., Shannon and fuzzy entropy based evolutionary image thresholding for image segmentation, Alexandria Engineering Journal., 2017

[28] Ye Z.W., Wang M. W., Liu W., Chen SB., Fuzzy entropy based optimal thresholding using bat algorithm, Applied Soft Computing., 2015, 31, 381-395

[29] Dice LR., Measures of the amount of ecologic association between species. Ecology, 1945, 26, 297-302

[30] JaccardP.,The distribution of the flora in the alpine zone. 1. New phytologist,1912,1,37-50

[31] Kumar R., Srivastava S., Srivastava R., A fourth order PDE based fuzzy c-means approach for segmentation of microscopic biopsy images in presence of Poisson noise for cancer detection, Computer methods and programs in biomedicine., 2017, 146, 59-68

[32] Sujan M., Alam N., Noman S. A., Islam M.J., A segmentation based Automated System for Brain Tumor Detection, International Journal of Computer Applications., 2016, 153,41-9

[33] Ilhan U., Ilhan A., Brain tumor segmentation based on a new threshold approach, Procedia Computer Science., 2017,120, 580-587